International Journal of Bioprinting

RESEARCH ARTICLE

# 3D printability and biochemical analysis of revalorized orange peel waste

**Jian Da Tan[1†], Cheng Pau Lee[1†], Su Yi Foo[2], Joseph Choon Wee Tan[2], Sakeena Si Yu Tan[1], Eng Shi Ong[2], Chen Huei Leo[2*], Michinao Hashimoto[1*]**

[1]Pillar of Engineering Product Development, Singapore University of Technology and Design, Singapore 487372, Singapore

[2]Science, Math & Technology, Singapore University of Technology and Design, Singapore 4787372, Singapore

(This article belongs to the *Special Issue: Related to 3D printing technology and materials*)

## Abstract

Orange peels are often discarded as food waste despite being a nutritious source of vitamins and antioxidants. These orange peel wastes (OPW) are produced in millions of tons globally every year; discarding them results in detrimental environmental and economical impacts. This paper discusses the application of 3D printing technology to effectively upcycle the OPW into edible, healthy snacks for consumption. We aimed to develop a method to enable OPW to formulate 3D-printable inks for direct ink writing (DIW). Using DIW 3D printing, we successfully created edible constructs of rheologically modified inks containing OPW. The formulated ink possessed an initial viscosity of 22.5 kPa.s, a yield stress of 377 Pa, and a storage modulus of 44.24 kPa. To validate the method, we conducted a biochemical analysis of the OPW at each stage of the fabrication process. This study suggested that our ink formulation and 3D printing process did not affect the content of bioflavonoids and antioxidants of the OPW. The cell viability test using human dermal microvascular endothelium (HMEC-1) suggested that the OPW did not exhibit cytotoxicity throughout the entire process of the ink manipulation. Overall, this study has highlighted a potential scenario to revalorize food waste into the food value chain using 3D printing toward more sustainable and circular food manufacturing and consumption.

***Keywords:*** 3D food printing; Direct ink writing; Circular economy; Orange peel waste; Food sustainability

[†]These authors contributed equally to this work.

***Corresponding authors:**
Michinao Hashimoto (hashimoto@sutd.edu.sg)

Chen Huei Leo (chenhuei_leo@sutd.edu.sg)

**Citation:** Tan JD, Lee CP, Foo SY, *et al*., 2023, 3D printability and biochemical analysis of revalorized orange peel waste. *Int J Bioprint,* 9(5): 776. https://doi.org/10.18063/ijb.776

**Received:** January 04, 2023
**Accepted:** February 23, 2023
**Published Online:** June 16, 2023



## 1. Introduction

This paper discusses 3D food printing based on direct ink writing (DIW) technology using orange peel waste (OPW). Millions of metric tons of oranges are produced each year globally, with nearly 30% by weight discarded as OPW[1]. The objective of this study is to demonstrate the ability of 3D printing to revalorize OPW to create edible snacks. Toward this end, we proposed to achieve four goals: (i) developing 3D printable inks comprising of OPW and appropriate additives, (ii) establishing the rheology of OPW inks, (iii) characterizing the biochemical properties before and after the printing process, and (iv) creating an edible snack using 3D printing. We successfully demonstrated the formulation of the 3D printable ink based on OPW using 1.0% w/w

xanthan gum. The formulated ink also maintained its antioxidant properties before and after printing. Our study demonstrated a simple method to recycle and reduce food waste toward food sustainability.

Citrus fruits, which are members the Rutaceas family, are among the most widely consumed and grown fruits in the world, with a report indicating production to have exceeded 130 million tons in 2015[2]. Among the various types of citrus fruits, the sweet orange (*Citrus sinensis* (L.) Osbeck) is a well-known source of natural antioxidants and certain phytochemicals (such as vitamin C and bioflavonoids) crucial for supporting nutrition and well-being[3]. According to projections for 2020/2021, orange production worldwide will rise to 49.4 million metric tons. It is anticipated that the quantity of OPW will increase concurrently with rising orange demand and consumption[4]. OPW is often recycled as animal feed, composted, or disposed of through incineration. To this end, it is beneficial to develop alternative ways to upcycle OPW to revalorize them back to the food value chain.

3D printing is a manufacturing technique which uses layer-by-layer deposition to create items. It has been used in numerous research areas, such as microfluidics[5-7], metal printing[8-10], and bioprinting[11-13]. In recent years, food printing has been widely demonstrated with DIW technology based on liquid extrusion. Customization of nutrients, creation of esthetically pleasing food, and changes to the internal structure of food are all made possible through 3D food printing[14-16]. Edible constructs with various internal structures provide distinctive textures during ingestion, which can be facilitated by the computer design of the 3D food model[17-19]. Thus, by modifying the mechanical properties of the printed meal, 3D food printing may offer prospective health benefits[20]. Chocolate[21], milk[22], mushroom[23], gelatin[24], and fish[25] are just a few examples of foods that have been used as ingredients in 3D food printing based on DIW. 3D food printing allows designing the mechanical properties and esthetics of the printed food, while it is crucial to ensure that the nutritional contents of the food are not compromised. Recent research has demonstrated that 3D food printing allows repurposing regularly discarded yet nutritious edible food byproducts like *okara*[26], potato peel[27], insect proteins[28], and grape pomace[29], enabling us to utilize them in our daily diets. DIW 3D printing requires multiple steps to handle the food materials (*e.g.*, ink formulation and extrusion). Despite the potential benefits of this approach, the impact of DIW 3D printing on the biochemical properties of food waste has not been studied carefully.

To bridge this gap, this work aimed to develop a method to create 3D structures using OPW mixed with hydrocolloids. We explored the use of extrusion-based food printing as a method of food processing. In particular, this work focused on characterizing (i) printability of the inks arising from their rheological properties and (ii) key biochemical properties at three critical stages of food processing (*i.e.*, ink preparation and extrusion printing). The usage of orange peels in 3D printable inks has previously been demonstrated as a nutritional supplement additive, with the orange peel containing 0.8% of the ink[30]. In this work, we intend to demonstrate the use of the OPW as the bulk printing material. We successfully formulated OPW inks with 0.4%–1.0% xanthan gum. Our rheological characterization suggested that the printable OPW ink with 1.0% xanthan gum possessed a yield stress of 377 Pa and a storage modulus of 44 kPa. Using this ink, we characterized the biochemical properties of the OPW at three critical stages during the fabrication: (i) powder, (i) ink, and (iii) print. Our characterization suggested that the formulation of the ink and printing did not affect the content of bioflavonoids and antioxidants of the OPW. The cell viability test using human dermal microvascular endothelium (HMEC-1) suggested that the OPW did not exhibit cytotoxicity throughout the entire process of the ink manipulation. While this work used OPW as an example of an underutilized fruit waste, the principles and methods discussed in this work should apply to other edible food waste for DIW 3D food printing.

## 2. Materials and methods

### 2.1. Nomenclature

To distinguish the formulations between the inks, the samples were labeled as a percentage of OPW powder and a percentage of xanthan gum in the deionized water. For example, the ink containing 20% w/w of OPW mixed with 0.4% w/w xanthan gum was labeled as O20XG4. Unless otherwise noted, this nomenclature was used throughout this paper.

### 2.2. Preparation of orange peel inks

OPW and deionized water were used to formulate OPW inks. Fresh OPW was collected from a fruit juice vendor (Uglyfood, Singapore) as food waste. The OPW was then dried in an oven heated at 60°C for 24 h. Dried OPW was ground into OPW powder using a 2000-W kitchen blender at 28000 rpm for 10 min. Next, the OPW powder was sifted using a 300-μm sieve (Industrial and Laboratory Consumables, China). OPW ink samples were prepared by adding OPW powder into deionized water containing xanthan gum at different formulations between 0.4% and 1.0% (*e.g.*, O20XG4, O20XG6, O20XG8, and O20XG10). All food inks were mixed thoroughly with a planetary centrifugal mixer (Thinky

ARE-250, Thinky Corporation, Tokyo, Japan) for 5 min at 2000 rpm at 25°C.

### 2.3. Rheological characterization

The oscillatory rheometer (Discovery Hybrid Rheometer DHR-2, TA Instruments, Delaware, USA) was used to measure the rheological properties of OPW inks. Stainless steel parallel plates with a diameter of 20 mm and a truncation gap of 500 μm were used for all measurements. Viscosity tests were conducted by applying a stepwise shear rate ramp from 0.01 to 1000 $s^{-1}$. To assess the viscoelastic properties of the samples, stress sweep measurements were performed with a logarithmically increasing shear stress at a constant frequency of 1 Hz over the range of 0.1–4000 Pa. Excess material outside the parallel plates was removed before measurements to prevent the edge effect. All rheological measurements were conducted at room temperature on triplicates.

### 2.4. DIW 3D printing

A pneumatic extrusion-based DIW printer (SHOTmini 200 Sx, Musashi Engineering, Inc., Tokyo, Japan) was used to print 3D models. MuCAD V software (Musashi Engineering, Inc., Tokyo, Japan) was used to control the speed and printing path of the DIW printer. Solidworks (Dassault Systèmes, Waltham, MA, USA), a computer-aided design (CAD) software, was used to create a 3D model. The created 3D model was then exported from Solidworks as a standard tessellation language (STL) file, which was then loaded into Slic3r, open-source software that divides the model into layers and creates G-code for 3D printers. In Slic3r, the infill level was selected. A home-made Python programming script was used to convert the resulting G-code to MuCAD V code, which was then put onto the DIW printer. All samples were loaded into a 50-mL Luer lock dispensing syringe (V-S liquid control equipment, China) fitted with a 20-G nozzle (Birmingham Gauge) (V-S liquid control equipment, China). All substrates used in this work were pre-cleaned glass substrates (Matsunami Glass Ind., Ltd, Osaka, Japan). Before printing, the standoff distance between the substrate and nozzle was calibrated to the layer thickness (set at 0.40 mm) using a height feeler gauge (QST Express-01, China). Throughout the printing process, the printing speed and dispensing pressure were 30 mm/s and 0.160 MPa, respectively. All printings were conducted at room temperature in a chamber to maintain a sterile environment. The process is illustrated and with the photograph of the experimental printer setup (Figure 1).

### 2.5. Microscope imaging

The height of the two-layer grid patterns was evaluated using an optical microscope (VHX-7000N, Keyence, Osaka, Japan). The images were taken with a 40× magnification lens. Surface profiling and color map overlay were done using the original software developed for the microscope.

### 2.6. Extraction and liquid chromatography-mass spectrometry profiling of 3D-printed samples

About 0.1 g of orange peel powder and 0.5 g of ink and printed samples were weighed and extracted using methanol extraction[31,32]. Briefly, 15 mL of methanol was added into each tube and placed in a sonicator with a water bath, and subjected to sonication at high frequency for 30 min at 40°C[31,32]. Extracts were subsequently filtered and used for subsequent experiments through a 0.45-μm filter and deposited in vials for compound analysis in the auto-sampling rack[31,32]. Liquid chromatography-mass spectrometry (LC/MS; Zorbax SB-C18 3.5 microns, 2.1 × 50 mm; Agilent, USA) was used to measure the level of flavonoids detected in the 3D-printed samples. The column temperature was kept at 40°C, and the total flow rate was fixed at 1.0 mL/min[32]. The injection volume was 10 μL, and it was separated concurrently in Nexera X-2 HPLC (Shimadzu, Japan) and LCMS-8050 LC-MS (Shimadzu, Japan)[30]. A mobile phase containing 0.1% formic acid in water and acetonitrile was used in the gradient elution[31,32]. The gradient parameter was calculated in a negative mode (M-H-) using the following conditions: 0.10 min at 10%, 15.00 min at 100%, 15.10 min at 10%, and 25.10 min at 10%; this condition was used to re-equilibrate the column to its starting settings[32]. The electrospray ionization mass spectrometry (ESI) was run with a 2.8 L/min nebulizing gas flow, a 300°C interface temperature, and a 9.0 L/min heating and drying gas flow[31,32]. Prior to getting an average reading for the three samples, the measured peak intensity for each sample was normalized to achieve a consistent sum[31,32].

### 2.7. Antioxidant capacity assays

The 1,1-diphenyl-2-picrylhydrazyl (DPPH) and azinobis-3-ethylbenzothiazoline-6-sulfonic acid (ABTS) assays were deployed in assessing the antioxidant capacity of the extracts obtained from 3D-printed samples. The principle of both assays allowed us to determine the antioxidant properties of the extracts by quantifying their ability to scavenge free radicals[31,33,34]. In the DPPH assay, the blank (200 μL of methanol), and 100 μL of extracts from orange peel powder, ink, and printed samples were transferred into the 96-well plate. Consequently, excluding the blank, 100 μL of 100 μM DPPH solution were added into each well for incubation at 25°C for 30 min[32]. All experiments were performed in triplicates. Ascorbic acid (10 mM) was used as the positive control for antioxidant scavenging activity[32]. For the ABTS assay, 88 μL of 140 mM potassium persulfate solution was added to 7 mM ABTS solution and the mixture was stored in the dark for 16 h[31]. This produced a dark purple-colored solution, consisting of ABTS•+,

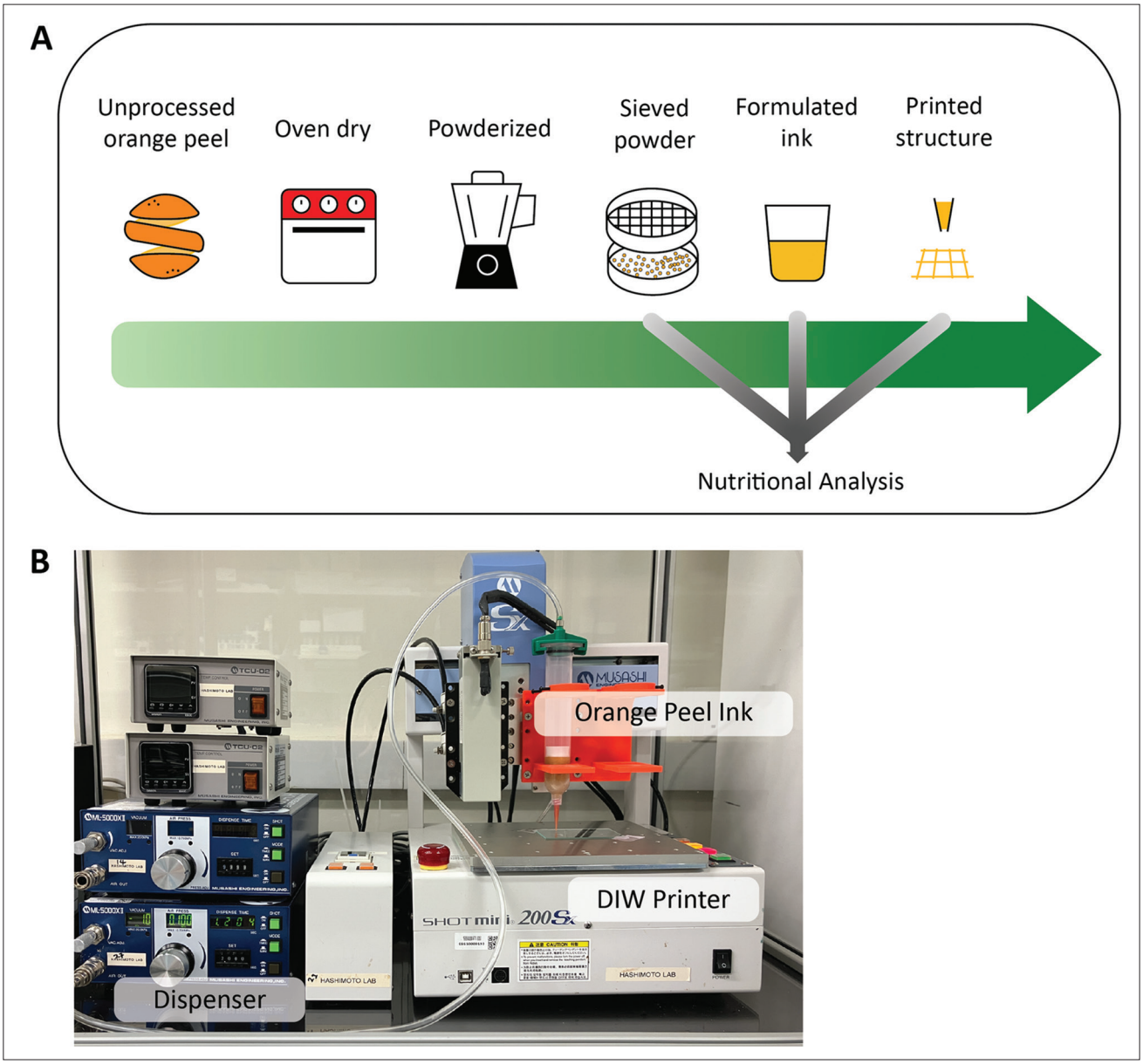


**Figure 1**. 3D printing of orange peel waste (OPW) by direct ink writing (DIW). (A) Flowchart describing the process to fabricate 3D-printable OPW inks and indication of nutritional analysis along the crucial steps of fabrication. (B) A photograph of a DIW 3D printer used in the experiment, equipped with a syringe attached to a pneumatic dispenser.

which was diluted with approximately 42.5 mL of methanol to give an initial absorbance of approximately 0.70–0.80 at 734 nm[35]. Ascorbic standard curve (100 µM–1 mM) was generated to produce 5%–50% inhibition of the blank absorbance (ABTS•+ alone) . Subsequently, 25 µL of extracts from orange peel powder, ink, and printed samples were added to the 96-well microplate containing 200 µL of ABTS•+ solution. All experiments were performed in triplicates[31]. The reaction was incubated for 30 min at 25°C with low-frequency shaking, and absorbance was measured at 734 nm using the Multiskan GO microplate reader (Thermo Scientific, Singapore)[31].

### 2.8. Cell viability

Human dermal microvascular endothelium (HMEC-1) cells were obtained (American Type Culture Collection [ATCC], USA) and cultured in MCBD-131 media (20% fetal bovine serum [FBS], 5% L-glutamic acid [200 mM], 1% penicillin-streptomycin and 0.001% recombinant human epidermal growth factor [EGF; 10 ng/mL]) using T75 flasks at 37°C, 5% $CO_2$[31,32]. At 75%–85% confluency, cells were seeded into cell-

cultured plate under serum-starved condition (2% FBS) and incubated for 24 h[32]. To evaluate the potential cytotoxicity effects induced by the extracts, 20 µL of extracts from orange peel powder, ink and printed samples was added to the cell culture medium and incubated for 24 h in 37°C, 5% $CO_2$ incubator[31,32]. The cells were monitored and observed for cell density and morphological alterations before determining cell viability by trypsinization and consecutively, cell counting[31]. The % cell viability was calculated using the formula, *i.e.*, $(C_S/C_B) \times 100\%$, where $C_S$ stands for the density of cells exposed to extracts and CB stands for the density of cells exposed to control (absence of methanol or extract)[31]. A total of five replicates were performed independently for each different treatment condition.

## 3. Results and discussion

### 3.1. Experimental design: Selection of material

The vast amount of OPW discarded globally is an issue worth addressing. Orange peel waste has been well studied to be consumable and nutritious, retaining an abundance of polyphenolic compounds such as flavonoids exhibiting antioxidant and anti-inflammatory properties[33]. These properties of OPW have been explored in intracellular oxidative stress studies, and the treatment of OPW on cells has been found to significantly reduce inflammatory biomarkers such as tumor necrosis factor alpha (TNFα), thereby reducing oxidative stress that primarily contributes to cellular dysfunction[33]. Despite these potential benefits, there have been few studies to 3D-print OPW with detailed attention to the influence on the biochemical properties, which should provide a solid basis to encourage the use of OPW to print health-beneficial snacks.

### 3.2. Formulation of inks

Sieving the blended OPW is a crucial step in creating printable inks as it prevents particles larger than the inner diameter of the printer's nozzle from causing a clog. The ink formulation from O20XG4 to O20XG10 contained mixtures of xanthan gum dispersed in deionized water at 0.4%, 0.6%, 0.8%, and 1.0%, respectively. The optical images showed a visual change in texture with increasingly large clumps formed along with the increase in the amount of xanthan gum added to the ink (Figure 2A). This observation was attributed to the increase in the adhesiveness of the ink by xanthan gum.

### 3.3. Rheological characterization

The measurement of the viscosity against shear rate suggested that all ink formulations (O20XG4, O20XG6, O20XG8, and O20XG10) exhibited shear thinning behavior (Figure 2B), which is desirable to perform DIW 3D printing of liquid-based materials. This characterization also suggested that the initial viscosity also decreased with an increasing amount of xanthan gum, with 36.9 kPa·s (O20XG4) and 22.5 kPa·s (O20XG10). This observation indicates that the granular particles within the ink can move one another easily with an increased amount of xanthan gum. The reduced frictional forces within the ink may result in a smooth mouthfeel once the material is 3D-printed. However, the overall values of the viscosity remained on the same order regardless the amount of xanthan gum, indicating there will be dominant factors that will determine the viscosity of the food inks (such as food concentrations and particle sizes).

The storage modulus ($G'$) and loss modulus ($G''$) relates to the ability of the viscous fluid to store energy elastically. Within the viscoelastic region where $G'$ is greater than $G''$, the ink behaves in an elastic manner (indicating that the ink is solid-like material). Beyond the point of intersection where $G'$ equals to $G''$, the ink will begin to deform inelastically and behave as a liquid-like material. This intersection point was used as an approximation for a yield stress of the formulated ink. From the $G'$ and $G''$ against oscillation stress graph, both the storage modulus and yield stress decreased with an increasing amount of xanthan gum added (Figure 2C). The storage modulus decreased from 53.19 kPa (O20XG4) to 44.24 kPa (O20XG10), while yield stress decreased from 680 (O20XG4) Pa to 377 Pa (O20XG10). This observation indicates that the addition of the xanthan gum to the ink lowers the solid-like mouthfeel. Crucially, the addition of the xanthan gum also decreases the pressure required to extrude the material from the ink barrel during the 3D printing The measured rheological properties are summarized (Table 1).

**Table 1. Values of initial viscosity, yield stress, storage moduli, and loss moduli obtained from the rheological analysis performed on four OPW inks**

| Fruit waste ink | Initial viscosity (kPa·s) | Yield stress (Pa) | Storage moduli (kPa) | Loss moduli (kPa) |
|---|---|---|---|---|
| **O20XG4** | 36.9 ± 5.17 | 680 ± 37 | 53.19 ± 0.24 | 8.40 ± 0.17 |
| **O20XG6** | 27.4 ± 0.73 | 514 ± 22 | 50.70 ± 0.34 | 8.38 ± 0.18 |
| **O20XG8** | 26.0 ± 0.68 | 429 ± 10 | 49.43 ± 0.24 | 8.84 ± 0.27 |
| **O20XG10** | 22.5 ± 1.41 | 377 ± 22 | 44.24 ± 0.56 | 8.10 ± 0.19 |

All values are expressed as mean ± standard deviation.

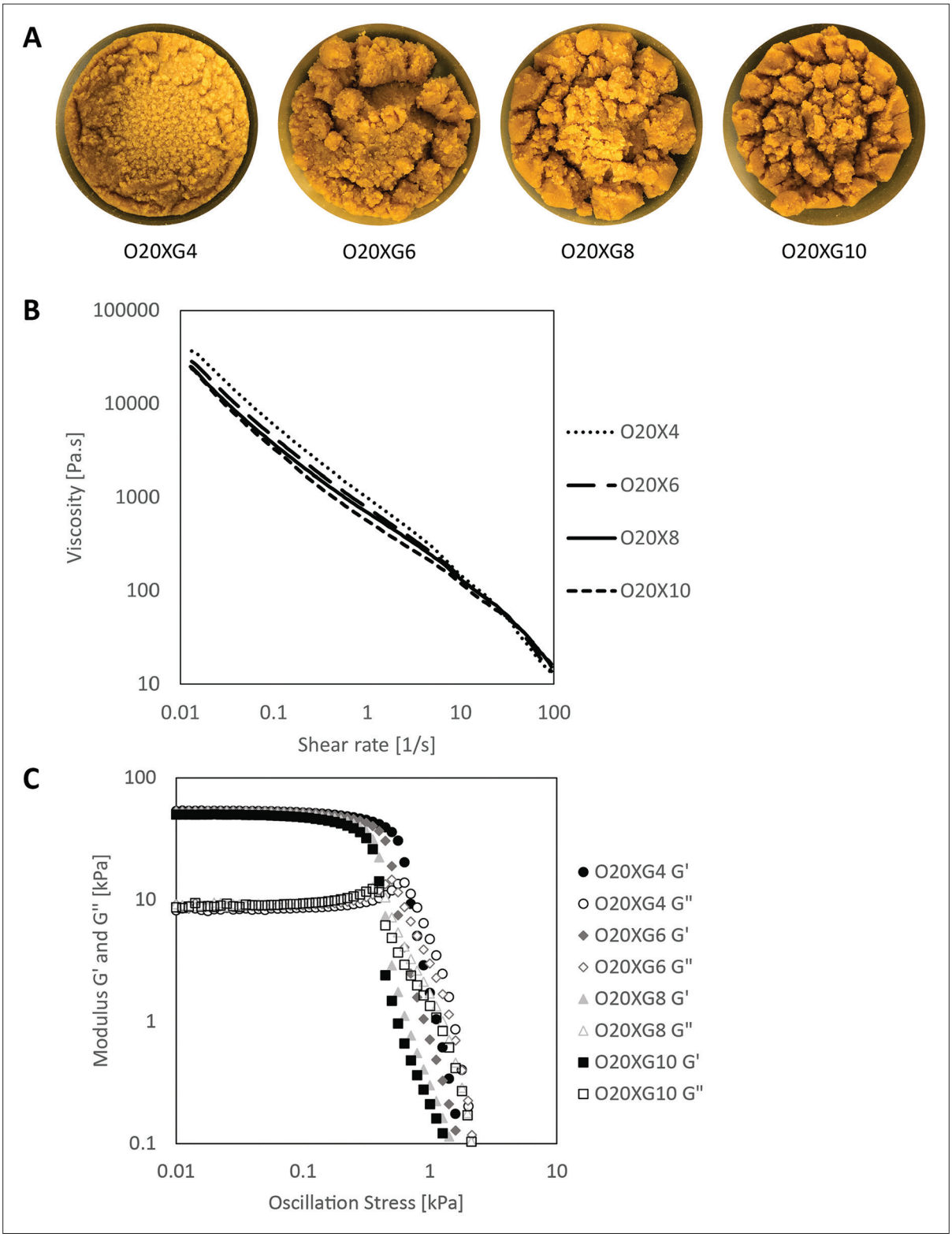


**Figure 2**. Formulation and rheology of OPW inks. (A) Optical images of the OPW inks with varying xanthan gum concentrations (0.4%, 0.6%, 0.8%, 1.0% w/w). (B) Plot showing the viscosity of OPW inks as a function of the applied shear rate. (C) Plot showing the storage and loss modulus as a function of the applied oscillatory shear stress.

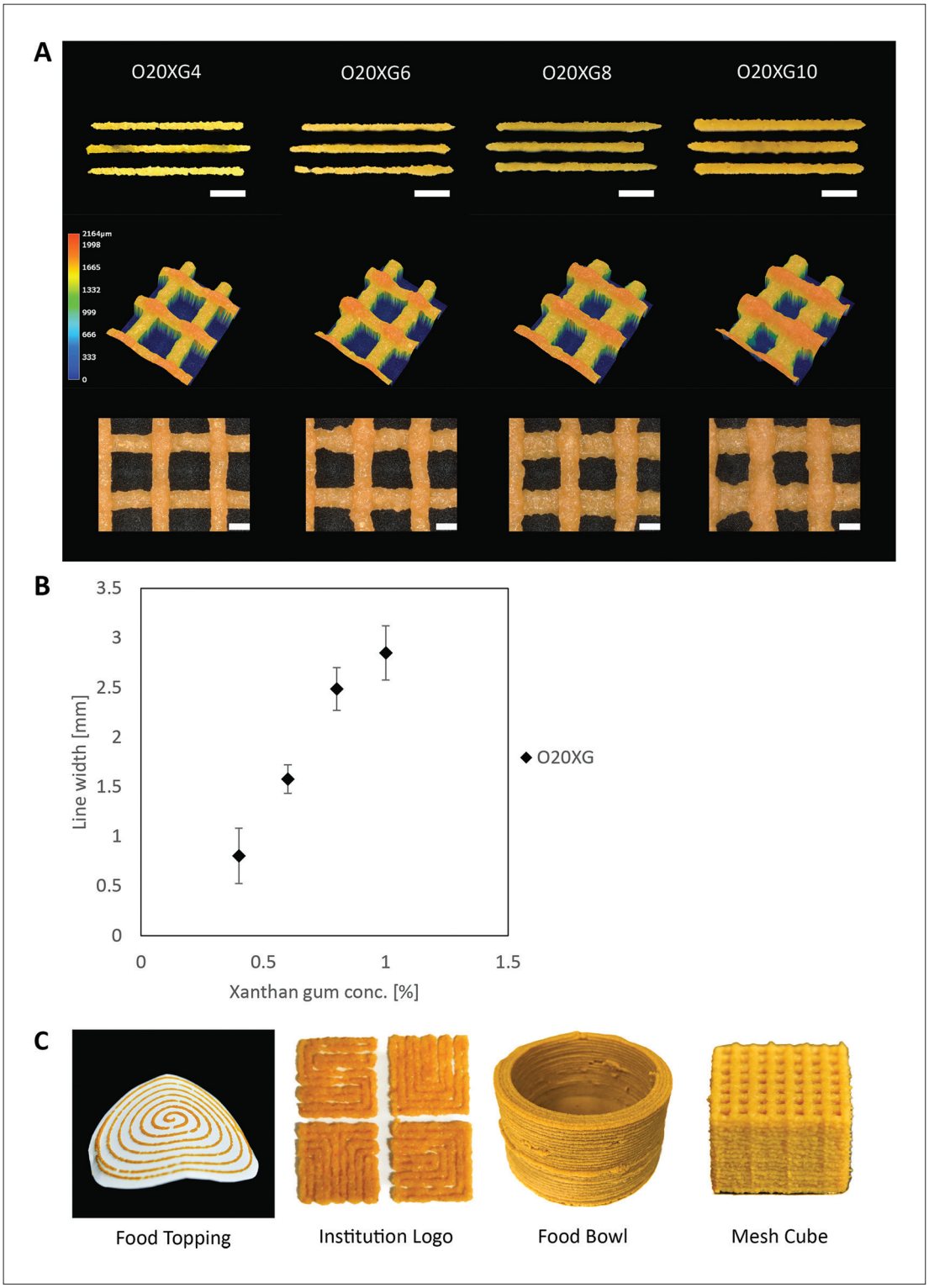


**Figure 3**. Characterization and demonstration of 3D-printed OPW inks by DIW. (A) Top: Optical images of the printed lines of the OPW inks with varying xanthan gum concentrations printed at constant pressure. Scale bar: 5 mm. Middle: Height map of the two-layer grid; the height of the printed structure is indicated by the colors, suggesting the sagging of the 2D grid for O20XG4 and O20XG6. The sample printed with O20XG10 did not exhibit noticeable sagging. Bottom: Optical images of two-layer grid pattern prints. Scale bar: 1 mm. (B) Plot showing the measured line width as a function of xanthan gum concentration in the ink after being extruded at a constant pressure. (C) Images of 3D-printed OPW inks demonstrated as food topping, logo display, food bowl, and mesh cube.

### 3.4. DIW printing

The printability of the inks was tested by printing distinct lines of 20 mm; the consistency and the continuity of the ink was characterized (Figure 3A). With a constant printing speed and extrusion pressure, the ease of extrusion was observed with an increase in xanthan gum concentration (Figure 3B). The line width increased from 0.8 mm to 2.8 mm for O20XG4 and O20XG10, respectively. The increasing line width indicated the increasing amount of material extruded, which is consistent with the Hagen–Poiseuille equation. Practically, a low extrusion pressure during printing is experimentally preferred as each instrument has maximum pressure that can be handled. This outcome is also in line with the measurement of the viscosity and the yield stress with respect to the xanthan gum concentration. To analyze the printability of the inks beyond the straight line, we printed two-layer grids to identify the structural integrity of the printed strut in the *z*-plane[36]. The inks between O20XG4 and O20XG8 exhibited various degrees of sagging within the overhang region. However, the color map indicated that O20XG10 demonstrated a solid printed line across the overhang region, potentially applicable to creating 3D structures (Figure 3A). These results suggested that O20XG10 was the most suitable formulation (among the inks we investigated) due to the formation of distinct and continuous lines at low pressure. We, therefore, used O20XG10 to print display pieces of 3D-printed OPWs (Figure 3C). Subsequently, O20XG10 was used to characterize their biochemical properties at different steps during DIW 3D printing.

### 3.5. Antioxidant capacity of OPW inks

The earlier results affirmed the capability to print 3D models of OPW. Thereafter, we characterized the biochemical properties of OPW at each step of 3D printing: (i) formation of the powder, (ii) formulation of the ink, and (iii) extrusion by DIW 3D printing. Orange peels are a rich source of naturally occurring bioactive compounds such as flavonoids and other polyphenolic compounds[33,34,37-39]. Previous studies have reported the abundance of two flavones (*i.e.*, hesperidin and narirutin) in orange peels[33,34,37-39]. Specifically, hesperidin (476.0 ± 8.6 mg/ 100 g of dry weight) and narirutin (241.3 ± 14.4 mg/ 100 g of dry weight) were measured as the highest yields in earlier studies[34,37,38]. These compounds are well reported for their health benefits due to their potent antioxidant[40,41] and anti-inflammatory activities[42-44]. Cardiovascular diseases are one of the leading causes of death worldwide, which are attributed to oxidative stress and chronic inflammation[45-47]. A recent study demonstrated that treatment of orange peel extract reversed TNFα-induced endothelial dysfunction *in vitro* primarily through anti-inflammatory action, suggesting the potential to upcycle the bioactive flavonoids from the orange peel, as a natural product, to target cardiovascular health benefits[34]. Hence, many studies have evaluated numerous natural products as potential treatment or prevention of chronic diseases such as cardiovascular diseases[48-50], diabetes[40,51], hypertension[52,53], and reproductive disorders[54,55]. While orange peel contains polyphenolic compounds, it remains unclear if 3D food printing affects the biochemical profile of the food product and the antioxidant activity. In this study, we measured the levels of narirutin and antioxidant capacity and compared them among three crucial stages of food printing (*i.e.*, powder, ink, and print). The narirutin levels of orange peel powder were comparable among the three stages (Figure 4). Similarly, the antioxidant capacity of orange peel powder was evaluated using the DPPH and ABTS assays (Figure 4B and C). It was evident that neither the formulation of food ink nor the 3D printing had a significant effect on the antioxidant capacity, which is characterized by their ability to scavenge free radicals. These experiments suggested that DIW printing did not change the antioxidant capabilities of the OPW while readily manipulating the physical properties and the structures of the OPW. These experiments also indicated that adding xanthan gum did not compromise the antioxidant capabilities originating from the OPW.

### 3.6. Cell culture and cell viability

Lastly, we evaluated the cytotoxicity of the OPW at the different stages of 3D food printing. We treated the cells with extracts from various 3D food processing stages for 24 h and observed the cell viability. The experiment suggested no significant differences in cell viability, morphological changes and/or contamination after exposure of cells to orange peel extracts from three different stages of food processing. DIW printing did not produce any potential cytotoxic substances detrimental to the cells (Figure 4D). Overall, 3D printing of OPW did not compromise the chemical composition of the food and its biological activity during the ink preparation and extrusion printing.

## 4. Conclusion

This paper presents the DIW 3D printing of OPW, which consists of sieved orange peel wastes mixed with xanthan gum. We characterized the rheological properties of the inks with various concentrations of xanthan gum; we identified O20XG10 as the most suitable for extrusion printing with an initial viscosity of 22.5 kPa, a storage modulus of 44.25 kPa, and a yield stress of 377 Pa. O20XG10 displayed the most distinct and continuous printed lines during the extrusion tests. LC/MS and cell viability analyses of the OPW powder and ink suggested that the entire process did not compromise

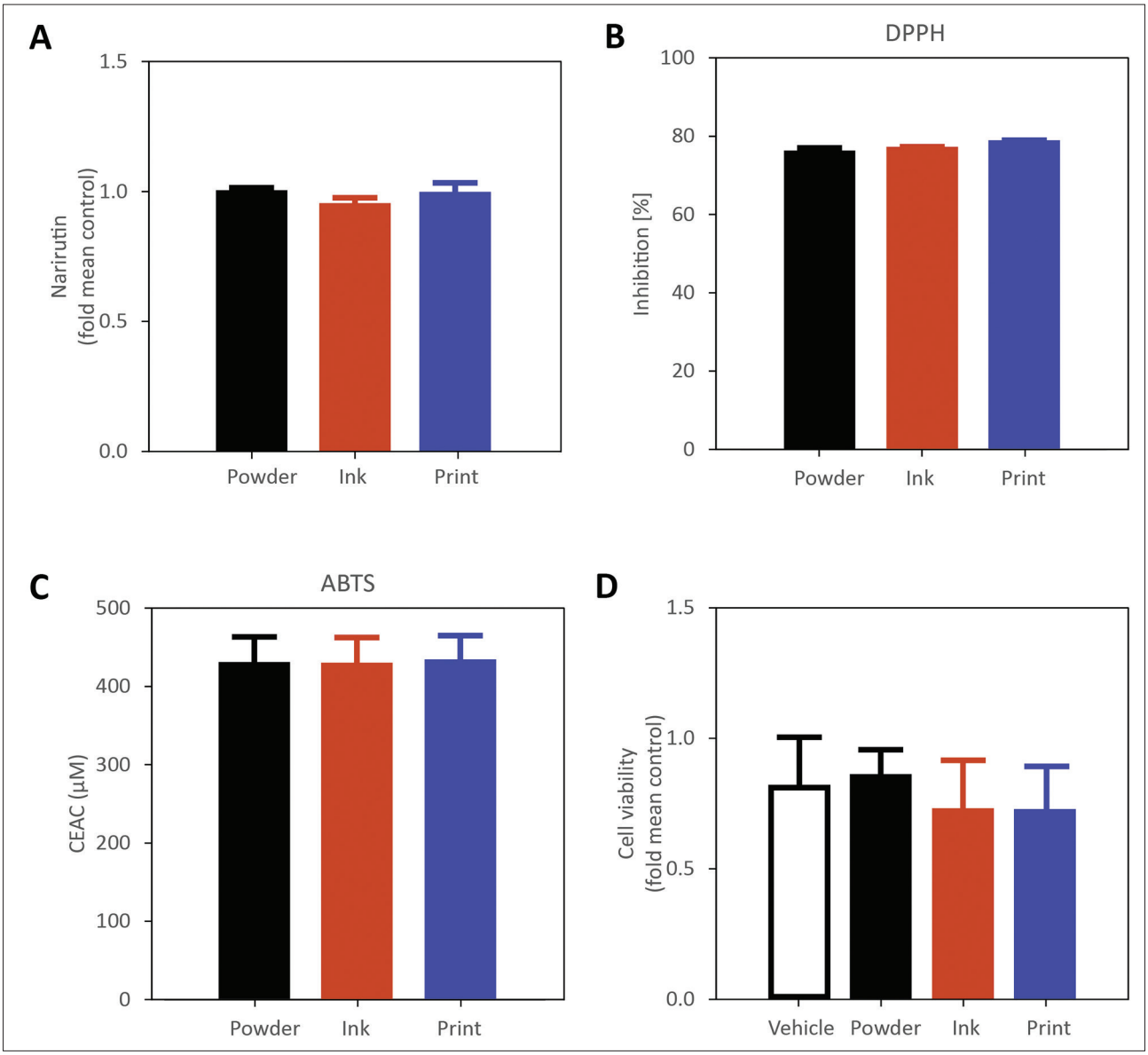


**Figure 4**. Biochemical analysis of the OPW at various stages of fabrication (dried powder, formulated ink, post-print). (A) LC/MS comparison of fold mean control narirutin levels at various stages of fabrication. (B) Antioxidant capacity in % inhibition determined by DPPH assay. (C) Antioxidant capacity in terms of vitamin C equivalent antioxidant capacity (CEAC) determined by ABTS assay. (D) Cell viability measured via fold mean control at three stages of 3D printing. Vehicle does not contain any OPW extract.

the biochemical profile of the ink. Further characterization by the DPPH and ABTS assays showed similar antioxidant activities before and after printing of the OPW ink.

This demonstration highlighted the revalorization of nutritious yet discarded fruit waste, which should pave an avenue to upcycle food waste and contribute to food sustainability. Given the original taste of OPW, it is necessary to develop a palatable taste of the final product (*i.e.*, an edible snack). Altering the taste of the 3D-printed food may be achieved with appropriate food additives and/or post-processing. In addition, while the primary objective of the presented study is to characterize the printability of the formulated ink, additional studies (including absorption of water, shape change by swelling, and formation of microstructures) remain to be performed to fully understand the properties of the printed foods. To ensure food safety, microbial testing should be performed before the 3D-printed foods can be served for consumption.

## Acknowledgments

C.P.L., J.D.T. and S.S.Y.T. acknowledged the financial support from the President's Graduate Fellowship and SUTD PhD Fellowship awarded by Ministry of Education (MOE), Singapore.

## Funding

M.H and C.H.L. acknowledge the project support by SUTD Growth Plan (SGP) in Healthcare Research (SGPHCRS1907), SUTD Kickstarter Initiative Grants (SKI 2021_02_05 and SKI 2021_02_09). C.H.L. acknowledges SUTD Start-up Research Grant (SRG-SMT-2020-156), and SUTD-ZJU Grant (ZJUVP2000102).

## Conflict of interest

The authors declare no conflict of interests.

## Author contributions

*Conceptualization*: Jian Da Tan, Cheng Pau Lee, Chen Huei Leo, Michinao Hashimoto

*Formal analysis*: Cheng Pau Lee, Jian Da Tan, Su Yi Foo, Joseph Choon Wee Tan, Sakeena Si Yu Tan

*Investigation*: Cheng Pau Lee, Jian Da Tan, Su Yi Foo, Joseph Choon Wee Tan, Sakeena Si Yu Tan

*Methodology*: Cheng Pau Lee, Jian Da Tan, Eng Shi Ong, Chen Huei Leo, Michinao Hashimoto

*Writing - original draft*: Cheng Pau Lee, Jian Da Tan, Chen Huei Leo, Michinao Hashimoto

*Writing - review & editing*: Cheng Pau Lee, Jian Da Tan, Chen Huei Leo, Michinao Hashimoto

## Ethics approval and consent to participate

Not applicable.

## Consent for publication

Not applicable.

## Availability of data

Data are available from the corresponding author upon reasonable request.

## References

1. Jiménez Nempeque LV, Gómez Cabrera AP, Colina Moncayo JY, 2021, Evaluation of Tahiti lemon shell flour (Citrus latifolia Tanaka) as a fat mimetic. *J Food Sci Technol*, 58(2):720–730.

2. Anticona M, Bleasa J, Frigola A, *et al.*, 2020, High biological value compounds extraction from citrus waste with non-conventional methods. *Foods*, 9:811.

   https://doi.org/10.3390/foods9060811

3. Pons E, Alquézar B, Rodríguez A, *et al.*, 2014, Metabolic engineering of β-carotene in orange fruit increases its in vivo antioxidant properties. *Plant Biotechnol J*, 12:17–27.

4. USDA, 2021, Citrus: World markets and trade. Available from:

   https://apps.fas.usda.gov/psdonline/circulars/citrus.pdf.

5. Ching T, Li Y, Karyappa R, *et al.*, 2019, Fabrication of integrated microfluidic devices by direct ink writing (DIW) 3D printing. *Sens Actuators B*, 297:126609.

6. Yamagishi K, Zhou W, Ching T, *et al.*, 2021, Ultra-deformable and tissue-adhesive liquid metal antennas with high wireless powering efficiency. *Adv Mater*, 33:2008062.

7. Sochol RD, Sweet E, Glick CC, *et al.*, 2018, *3D printed microfluidics and microelectronics. Microelectron Eng*, 189:52–68.

8. Jing Ll, Li YH, Cheng KW, *et al.*, 2020, Application of selective laser melting technology based on titanium alloy in aerospace products. *IOP Conf Ser: Mater Sci Eng*, 740:012056.

9. Van Der Merwe SR, Okanigbe DO, Desai DA, *et al.*, 2022, A review on impact resistance of partially filled 3D printed titanium matrix composite designed aircraft turbine engine fan blade, in TMS 2022 151st Annual Meeting & Exhibition Supplemental Proceedings, Springer.

10. Mami F, Revéret J-P, Fallaha S, *et al.*, 2017, Evaluating eco-efficiency of 3D printing in the aeronautic industry. *J Ind Ecol*, 21(S1):S37–S48.

11. De Santis MM, Alsafadi HN, Tas S, *et al.*, 2021, Extracellular-matrix-reinforced bioinks for 3D bioprinting human tissue. *Adv Mater*, 33:2005476.

12. Chansoria P, Shirwaiker R, 2019, Characterizing the process physics of ultrasound-assisted bioprinting. *Sci Rep*, 9(1):1–17.

13. Sriphutkiat Y, Kasetsirikul S, Ketpun D, *et al.*, 2019, Cell alignment and accumulation using acoustic nozzle for bioprinting. *Sci Rep*, 9(1):1–12.

14. Dankar I, Haddarah A, Omar FEL, *et al.*, 2018, 3D printing technology: The new era for food customization and elaboration. *Trends Food Sci Technol*, 75:231–242.

15. Lee CP, Hoo JY, 2021, Hashimoto M, Effect of oil content on the printability of coconut cream. *Int J Bioprint*, 7:354.

16. Liu Z, Bhandari B, Prakash S, *et al.*, 2018, Creation of internal structure of mashed potato construct by 3D printing and its textural properties. *Food Res Int*, 111:534–543.

17. Lee AY, Pant A, Pojchanun K, *et al.*, 2021, Three-dimensional printing of food foams stabilized by hydrocolloids for hydration in dysphagia. *Int J Bioprint*, 7:393.

18. Liu Z, Zhang M, 2021, Texture properties of microwave post-processed 3D printed potato snack with different ingredients and infill structure. *Future Foods*, 3:100017.

19. Mantihal S, Prakash S, Bhandari B, 2019, Texture-modified 3D printed dark chocolate: Sensory evaluation and consumer perception study. *J Texture Stud*, 50(5):386–399.

20. Liu Z, Bhandari B, Guo C, *et al.*, 2021, 3D printing of shiitake mushroom incorporated with gums as dysphagia diet. *Foods*, 10:2189.

21. Karyappa R, Hashimoto M, 2019, Chocolate-based ink three-dimensional printing (Ci3DP). *Sci Rep*, 9:14178.

22. Lee CP, Karyappa R, Hashimoto M, 2020, 3D printing of milk-based product. *RSC Adv*, 10:29821–29828.

23. Keerthana K, Anukiruthika T, Moses JA, *et al.*, 2020, Development of fiber-enriched 3D printed snacks from alternative foods: A study on button mushroom. *J Food Eng*, 287:110116.

24. Tan JJY, Lee CP, Hashimoto M, 2020, Preheating of gelatin improves its printability with transglutaminase in direct ink writing 3d printing. *Int J Bioprint*, 6:296.

25. Wang L, Zhang M, Bhandari B, *et al.*, 2018, Investigation on fish surimi gel as promising food material for 3D printing. *J Food Eng*, 220:101–108.

26. Lee CP, Takahashi M, Arai S, *et al.*, 2021, 3D printing of okara ink: The effect of particle size on the printability. *ACS Food Sci Technol*, 1:2053–2061.

27. Muthurajan M, Veeramani A, Rahul T, *et al.*, 2021, Valorization of food industry waste streams using 3D food printing: A study on noodles prepared from potato peel waste. *Food Bioproc Technol*, 14(10):1817–1834.

28. Zhang Y, Lee AY, Pojchanun K, *et al.*, 2022, Systematic engineering approach for optimisation of multi-component alternative protein-fortified 3D printing food Ink. *Food Hydrocolloids*, 131:107803.

29. Jagadiswaran B, Alagarasan V, Palanivelu P, *et al.*, 2021, Valorization of food industry waste and by-products using 3D printing: A study on the development of value-added functional cookies. *Future Foods*, 4:100036.

30. Maldonado-Rosas R, Tejada-Ortigoza V, Cuan-Urquizo E, *et al.*, 2022, Evaluation of rheology and printability of 3D printing nutritious food with complex formulations. *Addit Manuf*, 58:103030.

31. Ong ES, Oh CLY, Tan JCW, *et al.*, 2021, Pressurized hot water extraction of okra seeds reveals antioxidant, antidiabetic and vasoprotective activities. *Plants*, 10:1645.

    https://doi.org/10.3390/plants10081645

32. Ong ES, Pek CJN, Tan JCW, *et al.*, 2020, Antioxidant and cytoprotective effect of quinoa (Chenopodium quinoa Willd.) with pressurized hot water extraction (PHWE). *Antioxidants*, 9:1110.

    https://doi.org/10.3390/antiox9111110

33. Cheigh C-I, Chung E-Y, Chung M-S, 2012, Enhanced extraction of flavanones hesperidin and narirutin from Citrus unshiu peel using subcritical water. *J Food Eng*, 110:472–477.

34. Leo CH, Foo SY, Tan JCW, *et al.*, 2022, Green extraction of orange peel waste reduces TNFα-induced vascular inflammation and endothelial dysfunction. *Antioxidants*, 11:1768.

35. Venkatesan T, Choi Y-W, Kim Y-K, 2019, Effect of an extraction solvent on the antioxidant quality of Pinus densiflora needle extract. *J Pharm Anal*, 9(3):193–200.

36. Lee JM, Yeong WY, 2020, Engineering macroscale cell alignment through coordinated toolpath design using support-assisted 3D bioprinting. *J R Soc Interface*, 17(168):20200294.

37. Leo CH, Lee CP, Foo SY, *et al.*, 2022, 3D printed nutritious snacks from orange peel waste. *Mater Today Proc*, In press.

    https://doi.org/10.1016/j.matpr.2022.08.484

38. Ong ES, Low J, Tan JCW, *et al.*, 2022, Valorization of avocado seeds with antioxidant capacity using pressurized hot water extraction. *Sci Rep*, 12:1–11.

39. Saini RK, Ranjit A, Sharma K, *et al.*, 2022, Bioactive compounds of citrus fruits: A review of composition and health benefits of carotenoids, flavonoids, limonoids, and terpenes. *Antioxidants*, 11:239.

40. Leo CH, Hart JL, Woodman OL, 2011, 3',4'-dihydroxyflavonol reduces superoxide and improves nitric oxide function in diabetic rat mesenteric arteries. *PLoS One*, 6:e20813.

    https://doi.org/10.1371/journal.pone.0020813

41. Ng HH, Leo CH, O'Sullivan K, *et al.*, 2017, 1,4-Anhydro-4-seleno-d-talitol (SeTal) protects endothelial function in the mouse aorta by scavenging superoxide radicals under conditions of acute oxidative stress. *Biochem Pharmacol*, 128:34–45.

42. Leo CH, Jelinic M, Ng HH, *et al.*, 2016, Serelaxin: A novel therapeutic for vascular diseases. *Trends Pharmacol Sci*, 37:498–507.

43. Leo CH Woodman OL, 2015, Flavonols in the prevention of diabetes-induced vascular dysfunction. *J Cardiovasc Pharmacol*, 65:532–544.

44. Marshall SA, Qin C, Jelinic M, *et al.*, 2020, The novel small-molecule annexin-A1 mimetic, compound 17b, elicits vasoprotective actions in streptozotocin-induced diabetic mice. *Int J Mol Sci*, 21:pii: E1384.

    https://doi.org/10.3390/ijms21041384

45. Kahlberg N, Qin C, Anthonisz J, *et al.*, 2016, Adverse vascular remodelling is more sensitive than endothelial dysfunction to hyperglycaemia in diabetic rat mesenteric arteries. *Pharmacol Res*, 111:325–335.

46. Li JC, Velagic A, Qin C, *et al.*, 2021, Diabetes attenuates the contribution of endogenous nitric oxide but not nitroxyl to endothelium dependent relaxation of rat carotid arteries. *Front Pharmacol*, 11:585740.

    https://doi.org/10.3389/fphar.2020.585740

47. Qin CX, Anthonisz J, Leo CH, *et al.*, 2020, NO• resistance, induced in the myocardium by diabetes is circumvented by the NO redox sibling, nitroxyl. *Antioxid Redox Signal*, 32:60–77.

48. Ng HH, Leo CH, Parry LJ, 2016, Serelaxin (recombinant human relaxin-2) prevents high glucose-induced endothelial dysfunction by ameliorating prostacyclin production in the mouse aorta. *Pharmacol Res*, 107:220–228.

49. Ng HH, Leo CH, Prakoso D, *et al.*, 2017, Serelaxin treatment reverses vascular dysfunction and left ventricular hypertrophy in a mouse model of type 1 diabetes. *Sci Rep*, 7:39604.

    https://doi.org/10.1038/srep39604

50. Leo CH, Fernando D, Tran L, *et al.*, Serelaxin treatment reduces oxidative stress and increases aldehyde dehydrogenase-2 to attenuate nitrate tolerance. *Front Pharmacol*, 8:141.

    https://doi.org/10.3389/fphar.2017.00141

51. Leo CH, Hart JL, Woodman OL, 2011, 3',4'-dihydroxyflavonol restores endothelium dependent relaxation in small mesenteric artery from rats with type 1 and type 2 diabetes. *Eur J Pharmacol*, 659:193–198.

52. Leo CH, Jelinic M, Ng HH, *et al.*, 2019, Recent developments in relaxin mimetics as therapeutics for cardiovascular diseases. *Curr Opin Pharmacol*, 45:42–48.

53. Leo CH, Ng HH, Marshall SA, *et al.*, 2020, Relaxin reduces endothelium-derived vasoconstriction in hypertension: Revealing new therapeutic insights. *Br J Pharmacol*, 177:217–233.

54. Langston-Cox A, Leo CH, Tare M, *et al.*, 2020, Sulforaphane improves vascular reactivity in mouse and human arteries after "preeclamptic-like" injury. *Placenta*, 101:242–250.

55. Marshall SA, Leo CH, Girling JE, *et al.*, 2017, Relaxin treatment reduces angiotensin II-induced vasoconstriction in pregnancy and protects against endothelial dysfunction. *Biol Reprod*, 96:895–906.